PHYSICAL REVIEW B VOLUME 60, NUMBER 21 1 DECEMBER 1999-I

Evolution with doping of the *ab*-plane infrared properties of $Bi_2Sr_2CaCu_2O_{8+\delta}$

N. L. Wang, A. W. McConnell, and B. P. Clayman
Department of Physics, Simon Fraser University, Burnaby, British Columbia, Canada V5A 1S6

(Received 22 February 1999)

A systematic optical study of well characterized, Y-substituted $Bi_2Sr_2CaCu_2O_{8+\delta}$ single crystals covering the range from optimal doping to the insulating phase is presented. Special attention is given to comparisons with two other prototype cuprate systems $La_{2-x}Sr_xCuO_4$ and $YBa_2Cu_3O_{7-\delta}$. It is emphasized that dynamical charge stripe correlations play an important role in governing the difference in optical response between these systems. [S0163-1829(99)04241-1]

I. INTRODUCTION

High-temperature superconductivity is obtained by chemically introducing charge carriers into quasi-two-dimensional antiferromagnetic insulators. During last few years single crystals with well controlled carrier concentrations have become available, which permit performance of various doping dependent measurements. Among them, infrared measurements provide fruitful information on charge excitations.

The most detailed doping dependent study of *ab*-plane infrared properties was performed on the $La_{2-x}Sr_xCuO_4$ (LSCO) (Ref. 1) and $YBa_2Cu_3O_{7-\delta}$ (YBCO) (Ref. 2) systems. Although both systems were found to exhibit similar transfers of spectral weight from charge-transfer insulator to low-energy excitations with doping, a remarkable difference was revealed between them. It was found that the plasma frequency was rather insensitive to doping for LSCO after samples entered the metallic region. In contrast, there is a considerable shift of the plasma frequency in YBCO as a function of oxygen content. The reason for the difference is still not clear.

It has been known for a long time that the doping level in $Bi_2Sr_2CaCu_2O_{8+\delta}$ (BSCCO) can be controlled by substituting Y or other rare-earth elements for Ca. Therefore this system provides a good choice for such study. However, optical studies of the effect of doping in this system have been neither detailed nor extensive as compared with LSCO or YBCO. The optical reflectance spectrum of Y-doped BSCCO was reported by Meada *et al.* on polycrystalline samples.[3] Information yielded from this early work was limited not only due to the polycrystalline effect but also because no Kramers-Kronig analysis was performed. Terasaki *et al.*[4] studied the optical spectra of a pure BSCCO crystal, a pure $Bi_2Sr_2YCu_2O_{8+\delta}$ crystal, and a $Bi_2Sr_2Ca_{0.5}Nd_{0.5}Cu_2O_{8+\delta}$ crystal. However, the Y or Nd concentrations in their samples were so high that the compounds were deeply in the insulating phase region. A very recent work was done by Itoh *et al.* on $Bi_2Sr_2Ca_{1-x}Y_xCu_2O_{8+\delta}$ films.[5] Unfortunately, their measurement did not include the far-infrared region from 100–1000 cm^{-1} (13 meV–0.13 eV). In addition, the reflection from the MgO substrate complicated the problem and made the analysis less reliable.

We have grown Y-doped BSCCO single crystals in the composition range from optimal doping to the insulating phase in the phase diagram.[6] We earlier reported on our investigation of the normal-state pseudogap and the superconducting gap in metallic samples by infrared measurements.[7] In the present work, we extend the infrared measurement to insulating sample. We concentrate on how the *ab*-plane optical spectra evolve with doping and compare them with LSCO and YBCO systems.

II. EXPERIMENT

Single crystals $Bi_2Sr_2Ca_{1-x}Y_xCu_2O_{8+\delta}$ with nominal $x=0$, 0.07, 0.11, 0.17 were grown by usual melting method.[6] X-ray-diffraction measurements verified that all crystals are the proper 2212 phase. The lattice parameter along the *c*-axis decreases monotonically from 30.86 Å for $x=0$ to 30.41 Å for $x=0.17$. The pure crystal ($T_c \approx 89$ K) as well as crystals with nominal Y content $x=0.07$ ($T_c \approx 70$ K) and 0.11 ($T_c \approx 30$ K) show metallic behavior in the normal state as evidenced by their resistivity. By contrast, the $x=0.17$ crystal exhibits insulating behavior in the normal state. A drop near 10 K in $\rho(T)$ related to the superconducting transition is seen, but zero resistance is not achieved above 4 K. Obviously, the carrier concentration in these samples decreases with Y substitution. Detailed descriptions of crystal growth, structure, and dc transport characterization can be found in the earlier report.[6] The optical reflectance measurements were performed on a Bruker IFS113V spectrometer from 50–9500 cm^{-1}. The reflectance has been extended to high frequency (40 eV) using the measurement of Terasaki *et al.*[4] The measurement and Kramers-Kronig analysis were done in the same way as described in Ref. 7.

III. EVOLUTION OF THE *ab*-PLANE SPECTRUM WITH DOPING

Figure 1(a) shows the measured reflectivity $R(\omega)$ at room temperature for the pure and Y-substituted samples. The spectra exhibit the well-known overdamped behavior, i.e., $R(\omega)$ drops steadily throughout the infrared region. With the substitution of Y for Ca, the spectra change dramatically. The magnitude of $R(\omega)$ decreases over a wide frequency range, thus greatly reducing the area under the reflectance curve. In addition, $R(\omega)$ changes its curvature from downward to upward as x increases.

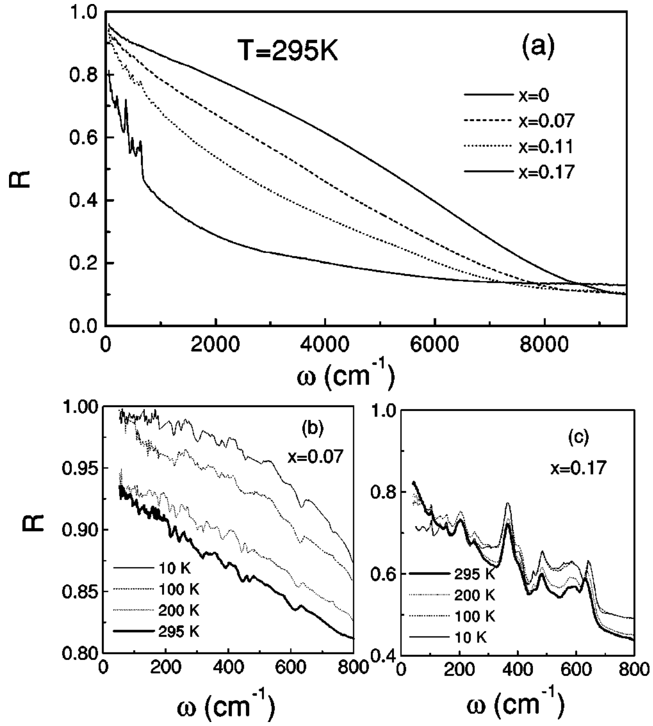

FIG. 1. (a) Doping dependence of the reflectivity at room temperature; (b) and (c): the far-infrared reflectivity for $x=0.07$ and $x=0.17$ samples at different temperatures.

Because of the overdamped nature of the spectrum, the screened plasma frequency cannot be determined from the measured reflectivity. However, the decrease of the low-ω reflectivity strongly suggests a reduction in plasma frequency. The phonon peaks become more prominent with Y substitution, which can be ascribed to the reduced screening effect from conducting carriers. Such spectral change is expected for a system with reduced carrier density. Actually, a metal-to-insulator transition can be inferred from the temperature dependence of the far-infrared (FIR) reflectivity of these samples. The FIR reflectivity increases with decreasing T for the pure and lightly Y-doped samples with $x=0.07$ and $x=0.11$, which is typical for a metallic response caused by reduced carrier scattering rate. As an example, Fig. 1(b) shows the spectra for $x=0.07$ sample. In contrast, the low-ω reflectivity of the heavily Y-doped $x=0.17$ sample [Fig. 1(c)] in the FIR region decreases with decreasing T, evidencing an insulating response. Thus the spectral change in these samples is consistent with the dc resistivity measurement showing a metal-to-insulator transition. Additionally, since the curvature of reflectance $R(\omega)$ is an indication of carrier damping, the change of $R(\omega)$ curvature demonstrates that the carrier damping is further enhanced by Y substitution.

The decrease of plasma frequency is reflected in the zero crossing of the real part of dielectric function and confirmed by the partial sum-rule of the conductivity. The real part of dielectric function $\epsilon_1(\omega)$ at room temperature, derived from the reflectivity spectra by Kramers-Kronig transformation, is illustrated as a function of doping in Fig. 2(a). There is a systematic shift of the zero crossing toward low frequency with increasing Y concentration. The result is contrast to the case of $La_{2-x}Sr_xCuO_4$ in which it was found that the zero crossing is pinned near 0.7 eV throughout a wide range in the metallic phase, $0.1 \leqslant x \leqslant 0.34$,[1] but is similar to the doping dependent behavior of YBCO.[2] According to the simple Drude model

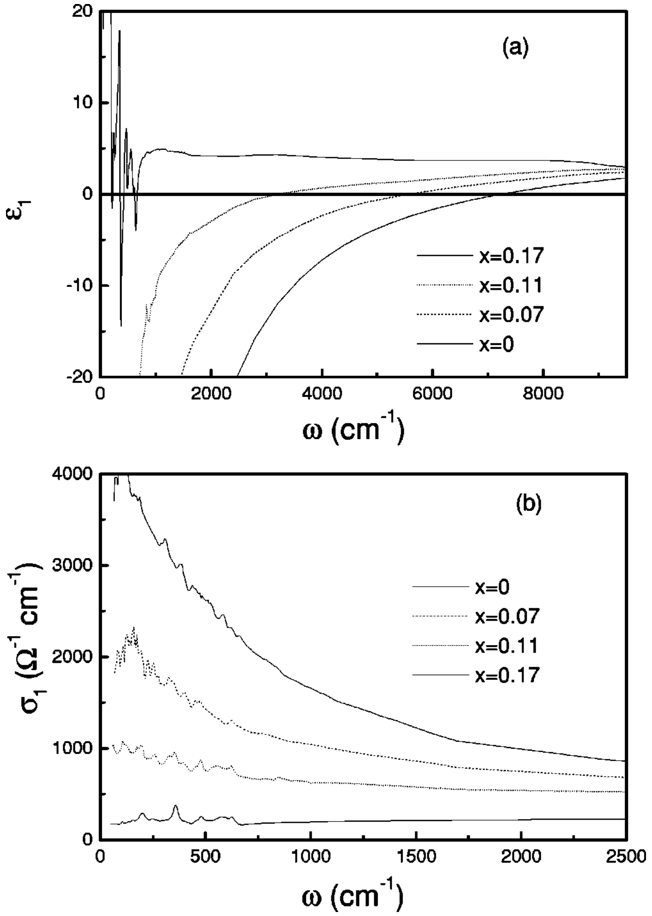

FIG. 2. The frequency-dependent real part of dielectric function (a) and conductivity (b) at room temperature.

$$\epsilon_1(\omega)=\epsilon_\infty-\omega_p^2/(\omega^2+1/\tau^2), \tag{1}$$

the zero crossing frequency ω_0 in $\epsilon_1(\omega)$ is related to the plasma frequency by $\omega_0^2=\omega_p^2/\epsilon_\infty-1/\tau^2$. For a simple metal with constant scattering rate, the zero crossing corresponds roughly to the screened plasma frequency $\omega_p'=\omega_p/\epsilon_\infty^{1/2}$. But for the overdamped cuprates, the crossing is also a function of damping. When the damping increases, the zero crossing also shifts to lower frequency. So, both the reduction of plasma frequency and the increase of damping contribute to this shift. For this reason, we cannot determine the screened plasma frequency uniquely from the zero crossing frequencies. For the $x=0.17$ sample, $\epsilon_1(\omega)$ is positive in the whole frequency region, except for effects due to phonons, which is consistent with insulating behavior.

The frequency-dependent conductivities at room temperature are shown in Fig. 2(b). The low-frequency spectral weight decreases systematically with Y doping, suggesting a decrease of free-carrier density. The conductivity of $x=0.17$ sample is very low at low frequency. Its magnitude decreases slightly with decreasing frequency, indicating nonmetallic conduction. This agrees well with the dc

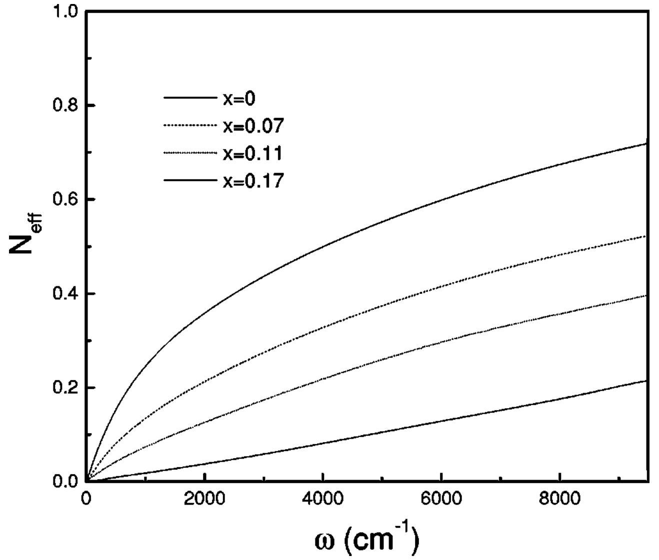

FIG. 3. Effective electron number per Cu atom calculated using the conductivity sum rule for various compositions.

measurement[6]. Actually, the reflectivity at high frequency for this sample connects better with Terasaki's data for $Bi_2Sr_2YCu_2O_{8+\delta}$ than with that of pure $Bi_2Sr_2CaCu_2O_{8+\delta}$.[4] For comparison, we performed the Kramers-Kronig transformation using both sets of high-frequency data, and found that the conductivity spectra are nearly identical below 5000 cm^{-1}. The main difference appears at frequencies higher than 9500 cm^{-1}. The missing low-ω spectral weight in Y-substituted samples must have been transferred to higher frequencies, which is believed to be a general phenomenon in cuprate superconductors.[8]

The effective density of carriers contributed to conductivity below ω can be calculated by the partial sum rule

$$N_{eff}(\omega)=\frac{2mV_{cell}}{\pi e^2}\int_0^{\omega}\sigma_1(\omega')d\omega', \qquad (2)$$

where V_{cell} is a unit cell volume. Figure 3 shows N_{eff} as a function of frequency for the four samples. It indicates clearly that the spectral weight decreases remarkably as samples evolve towards insulating behavior.

N_{eff} can be related to an equivalent plasma frequency, after choosing a proper high-frequency limit ω_c, via the relationship $\omega_p^2=4\pi e^2N_{eff}(\omega_c)/mV_{cell}=8\int_0^{\omega_c}\sigma_1(\omega')d\omega'$. Obviously, there is an uncertainty associated with the choice of the high-frequency cutoff limit. In fact, determination of the plasma frequency depends greatly on the choice of a one-component or two-component approach, an issue raised long ago but still not yet resolved.[9] Recent studies tend to favor the one-component description of the charge dynamics.[10,7] Choosing $\omega_c=1$ eV, a frequency where $\sigma_1(\omega)$ almost reaches its minimum but below the charge transfer gap energy, we get $\omega_p=1.67\times10^4$ cm^{-1} for the pure sample, 1.42×10^4 cm^{-1} for $Y=0.07$, 1.22×10^4 cm^{-1} for $Y=0.11$, and 0.86×10^4 cm^{-1} for $Y=0.17$. It should be pointed out that, if one uses a two-component picture, the plasma frequencies are overestimated since they include some contributions from bound carriers. However, because the spectral weight increases even more rapidly at low frequency (Fig. 3), we are certain that the plasma frequency increases with doping. This is different from the LSCO system in which the plasma frequency is almost independent of doping.[1]

Another important quantity which can be determined easily from the one-component approach is the carrier scattering rate, or damping. For the three metallic samples, the scattering rates were extracted from the extended Drude model analysis and presented in Ref. 7.[11] It can be seen clearly that the room-temperature scattering rate increases with Y substitution, evidencing the further enhancement of carrier damping.

IV. DISCUSSION

The evolution of the spectra with increasing Y substitution presented above reveals two main effects: a decrease of plasma frequency and an enhancement of carrier damping. In the previous studies, there is some controversy about whether or not the plasma frequency changes with doping. One view is that the plasma frequency is associated with the reflectivity minimum (edge) which varies widely for different cuprate materials but does not change appreciably with doping in each system.[9] The present result thus argues against this opinion. In fact, because of overdamped nature, the reflectivity edge cannot be readily determined from Fig. 1(a), especially for samples with further reduced carrier concentrations. We believe that for overdamped materials the reflectivity minimum does not reflect well the (screened) plasma frequency.

We note that the large change of plasma frequency with doping in this system appears similar to what occurs in YBCO with a change of oxygen content,[2] but is in sharp contrast to the situation in LSCO.[1] This observation points to the essential difference in electronic states between these systems. It is of great interest to unravel the reasons for the difference.

As realized previously, compared to optimally doped BSCCO or YBCO, a notable difference in the *ab*-plane response of LSCO is a pronounced enhancement of the mid-infrared (MIR) conductivity.[2,12] For lightly doped compositions in the LSCO materials, the *ab*-plane conductivity spectrum exhibits two distinct parts: a Drude-like part at low frequency and a MIR absorption feature. Though the MIR absorption shifts its position and merges into the Drude-like absorption with increasing doping,[1] it remains relatively high. By contrast, the MIR absorption is much weaker and cannot be unambiguously resolved in the BSCCO and YBCO ($\mathbf{E}\|\mathbf{a}$) materials. Therefore the question remains about the origin of the MIR absorption, especially as to the reason that LSCO has enhanced conductivity in the MIR region.

In fact, the origin of the MIR absorption has been an issue from the beginning of the discovery of high-T_c superconductivity.[8,9] The MIR absorption was explained as due to the incoherent motion of doped carriers in the background of antiferromagnetic spin fluctuation based on *t*-*J* model.[13–15] Alternatively, the absorption was assigned to a separate band contributed by bound carriers in terms of the two-component picture.[8,9] A new insight is to relate the enhanced MIR absorption to the dynamic charge stripes.[12] Up to now, static charge stripes in cuprates have been only observed in Nd-substituted LSCO owing to the stabilization of low-T tetragonal structure.[16] It was found that Nd substitution leads to a suppression of the low-ω ab-plane conductivity, even at temperatures much higher than the static stripe ordering temperature; this results in a relative enhancement of conductivity in the MIR region.[12,17] The observation was explained by strong fluctuations of the stripes at high temperatures. Since the MIR conductivity is enhanced in pure LSCO relative to BSCCO or YBCO, it is speculated that even the pure LSCO is affected by such stripe fluctuations.[12]

The interpretation based on fluctuating charge stripes is particularly plausible since it can be reconciled with other studies[18–21] showing that strong dynamic stripe correlations exist in pure LSCO material within a wide range of doping levels. For example, a recent angle-resolved photoemission spectroscopy (ARPES) measurement[21] revealed broad, weak spectral weight near $(\pi/2, \pi/2)$ along the $(0,0)$-(π,π) direction in LSCO. This feature is very different from BSCCO, where a sharp peak is seen. The suppression of the low-energy excitation near $(\pi/2,\pi/2)$ in LSCO was ascribed to the insulating property in the direction crossing the charge stripes, since the stripes seen via neutron-scattering measurements[16] are oriented along $(0,0)$-$(\pi,0)$ or $(0,0)$-$(0,\pi)$ directions.

Recently, a theoretical study of the effect of charge stripes on $\sigma_1(\omega)$ was carried out by Tohyama *et al.* based on t-t'-t''-J model.[22] They showed that not only the charge carriers moving perpendicular to the stripes contribute an incoherent (or MIR) weight to $\sigma_1(\omega)$, but those moving along the stripes also contribute, in addition to a Drude weight, a sizable incoherent weight. Their calculations confirmed the enhancement of the MIR conductivity by charge stripes. Given that dynamic charge stripes exist for a wide range of doping levels in LSCO, we expect that the increase in Drude weight with dopant concentration would be small with respect to the large spectral weight in the MIR region; as a result, the plasma frequency does not change appreciably with doping.

Finally, we discuss briefly the question of whether the plasma frequency is correlated with the lattice parameter. Previously, to account for the fact that different materials have different plasma frequencies, Tajima *et al.* investigated the possible relationship between lattice parameters and plasma frequencies by examining a number of materials with different CuO_2 layers in a unit cell. They found that plasma frequencies scaled roughly with the inverse of the average interplane spacing $d = c/N$, where c is the lattice parameter along c axis and N the number of the CuO_2 planes in a unit cell.[23] However, the present series are opposite to this trend, since both the plasma frequency and c-axis lattice parameter decrease with Y substitution. The diversity of these observations implies that plasma frequency is a quantity which is not correlated with structural parameters. We conclude that the plasma frequency does change appreciably with the doping level in cuprate superconductors, but consider the LSCO system an exception caused presumably by the particularly strong dynamic stripe correlations.

In summary, we have performed a systematic optical study on Y-substituted $Bi_2Sr_2CaCu_2O_{8+\delta}$, concentrating on the evolution of ab-plane optical spectrum with doping. The study reveals two main effects: decrease of plasma frequency and further enhancement of carrier damping. The results were compared with other propotype cuprate systems LSCO and YBCO. It is emphasized that dynamical stripe correlations play an important role in determining the different properties of these systems. In particular, the pinning of the plasma frequency in LSCO is considered to be an exceptional case. It is linked with the enhanced mid-infrared absorption being caused by the particularly strong dynamic stripe correlations.

This work was supported by grants from the NSERC and Simon Fraser University.

---

[1] S. Uchida, T. Ido, H. Takagi, T. Arima, Y. Tokura, and S. Tajima, Phys. Rev. B **43**, 7942 (1991).

[2] S. L. Cooper, D. Reznik, A. Kotz, M. A. Karlow, R. Liu, M. V. Klein, B. W. Veal, and A. P. Paulikas, Phys. Rev. B **47**, 8233 (1993).

[3] A. Maeda, M. Hase, I. Tsukada, K. Noda, S. Takebayashi, and K. Uchinokura, Phys. Rev. B **41**, 6418 (1990).

[4] I. Terasaki, T. Nakahashi, S. Takebayashi, A. Maeda, and K. Uchinokura, Physica C **165**, 152 (1990).

[5] T. Itoh, K. Fueki, Y. Tanaka, and H. Ihara, J. Phys. Chem. Solids **60**, 41 (1999).

[6] N. L. Wang, B. Buschinger, C. Geibel, and F. Steglich, Phys. Rev. B **54**, 7445 (1996).

[7] N. L. Wang, A. W. McConnell, B. P. Clayman, and G. D. Gu, Phys. Rev. B **59**, 576 (1999).

[8] See review article, D. B. Tanner, and T. Timusk, in *Physical Properties of High Temperature Superconductors III*, edited by D. M. Ginsberg (World Scientific, Singapore, 1992), p. 339.

[9] See review article, S. Tajima, Supercond. Rev. **2**, 125 (1997).

[10] T. Timusk, A. V. Puchkov, D. N. Basov, and T. Startseva, J. Phys. Chem. Solids **59**, 1953 (1998).

[11] Because the $x = 0.17$ sample is not metallic, it is meaningless to attempt to derive it from this model.

[12] S. Tajima, N. L. Wang, N. Ichikawa, H. Eisaki, S. Uchida, H. Kitano, T. Hanaguri, and A. Maeda, Europhys. Lett. **47**, 715 (1999).

[13] T. M. Rice and F. C. Zhang, Phys. Rev. B **39**, 815 (1989).

[14] A. Moreo and E. Dagotto, Phys. Rev. B **42**, 4786 (1990).

[15] W. Stephan and P. Horsch, Phys. Rev. B **42**, 8736 (1990).

[16] J. M. Tranquada, B. J. Sternlieb, J. D. Axe, Y. Nakamura, and S. Uchida, Nature (London) **375**, 561 (1995); J. M. Tranquada, J. D. Axe, N. Ichidawa, A. R. Moodenbaugh, Y. Nakamura, and S. Uchida, Phys. Rev. Lett. **78**, 338 (1997); J. M. Tranquada, J. D. Axe, N. Ichidawa, Y. Nakamura, S. Uchida, and B. Nachumi, Phys. Rev. B **54**, 7489 (1996).

[17] S. Tajima, N. L. Wang, M. Takaba, N. Ichikawa, and S. Uchida, J. Phys. Chem. Solids **59**, 2015 (1998).

[18] S. R. White and D. J. Scalapino, Phys. Rev. Lett. **81**, 3227 (1998).

[19] A. Bianaconi, N. L. Saini, A. Lanzara, M. Missori, T. Rossetti, H. Oyanagi, H. Yamaguchi, K. Oka, and T. Ito, Phys. Rev. Lett. **76**, 3412 (1996).

[20] M. I. Salkala, V. J. Emery, and S. A. Kivelson, Phys. Rev. Lett. **77**, 155 (1997).

[21] A. Ino, C. Kim, M. Nakamura, T. Mizokawa, Z. X. Shen, A. Fujimori, T. Kakeshita, H. Eisaki, and S. Uchida, cond-mat/9902048 (unpublished).

[22] T. Tohyama, S. Nagai, Y. Shibata, and S. Maekawa, Phys. Rev. Lett. **82**, 4910 (1999).

[23] S. Tajima, S. Uchida, T. Kaneko, I. Tomeno, M. Kosuge, H. Yamauchi, and N. Koshizuka, Physica C **194**, 301 (1992).